Science & Technology Facilities Council

Technical Report
RAL-TR-2017-007

The problem of lost neutron flux on the MAPS instrument, and how it was recovered

RA Ewings, TG Perring, RC Riehl-Shaw, EL Johnson, SR Wakefield, G Skoro, D Raspino, SR Moorby, P Phillips, DD Abbley, DJ Haynes, SP Waller, RI Bewley, JR Stewart

July 2017

Enquiries concerning this report should be addressed to:

RAL Library
STFC Rutherford Appleton Laboratory
Harwell Oxford
Didcot
OX11 0QX

Tel: +44(0)1235 445384
Fax: +44(0)1235 446403
email: libraryral@stfc.ac.uk

Science and Technology Facilities Council reports are available online at: http://epubs.stfc.ac.uk

ISSN 1358-6254

The problem of lost neutron flux on the MAPS instrument, and how it was recovered

R. A. Ewings, T. G. Perring, R. C. Riehl-Shaw, E. L. Johnson, S. R. Wakefield, G. Skoro, D. Raspino, S. R. Moorby, P. Phillips, D. D. Abbley, D. J. Haynes, S. P. Waller, R. I. Bewley and J. R. Stewart

31.07.2017

Abstract

After a long ISIS shutdown on target station 1 during 2016, it was found that the neutron flux on the MAPS spectrometer was substantially compromised, with an energy-dependent reduction of between two and five measured. To determine and remedy the cause of this problem, extensive investigations were performed, both on the instrument and involving neutronic and ray-tracing simulations. The key measurement that provided the most insight into the nature of the problem was to use a pinhole camera setup to obtain a spatially-resolved image of the neutron source as viewed from the sample. This revealed a highly inhomogeneous distribution of flux from the source, in contrast to a similar measurement performed on the adjacent VESUVIO beamline which views the same moderator face but showed no such inhomogeneity. The problem was eventually solved by replacing the MAPS beamline shutter, an expensive and difficult task.

Introduction

At the start of ISIS beam cycle 16/3, after a long shutdown on target station 1 (TS-1) between May and September 2016, it was observed during standard calibrations that the flux on the MAPS instrument was substantially lower than normal. Initial characterisation of the reduced flux was an attenuation of around a factor of two at the higher neutron energy end of MAPS' operating region, and a factor of five at the lower neutron energy end. Such reductions in flux had a major impact on the user programme, resulting in the cancellation of approx. 50% of scheduled experiments (largely those requiring lower neutron energies) and longer measurement times were required for the remainder.

The aim of this report is to document all of the diagnostic tests and interventions that were performed on MAPS. It is hoped that, should similar problems ever occur on another instrument, this can be used as a successful recipe for their satisfactory resolution.

Characterisation

Figure 1 below shows data from a typical calibration measurement performed on MAPS, when the instrument is operating properly. For these measurements a flat plate vanadium standard sample is used with the instrument in white beam mode, i.e. with the Fermi chopper removed. The detector tank is evacuated to <1 mbar, more typically ~5×10^{-6} mbar, to eliminate a contribution to the signal from air scattering. The spectra from the first 512 detector elements, in the A1 forward detector bank, are summed to produce the data shown in panel (c). Similar measurements are also obtained from the monitors,

located between the t-zero and Fermi choppers (monitor 1, panel (a)) and just after the Fermi chopper (monitor 2, panel (b)).

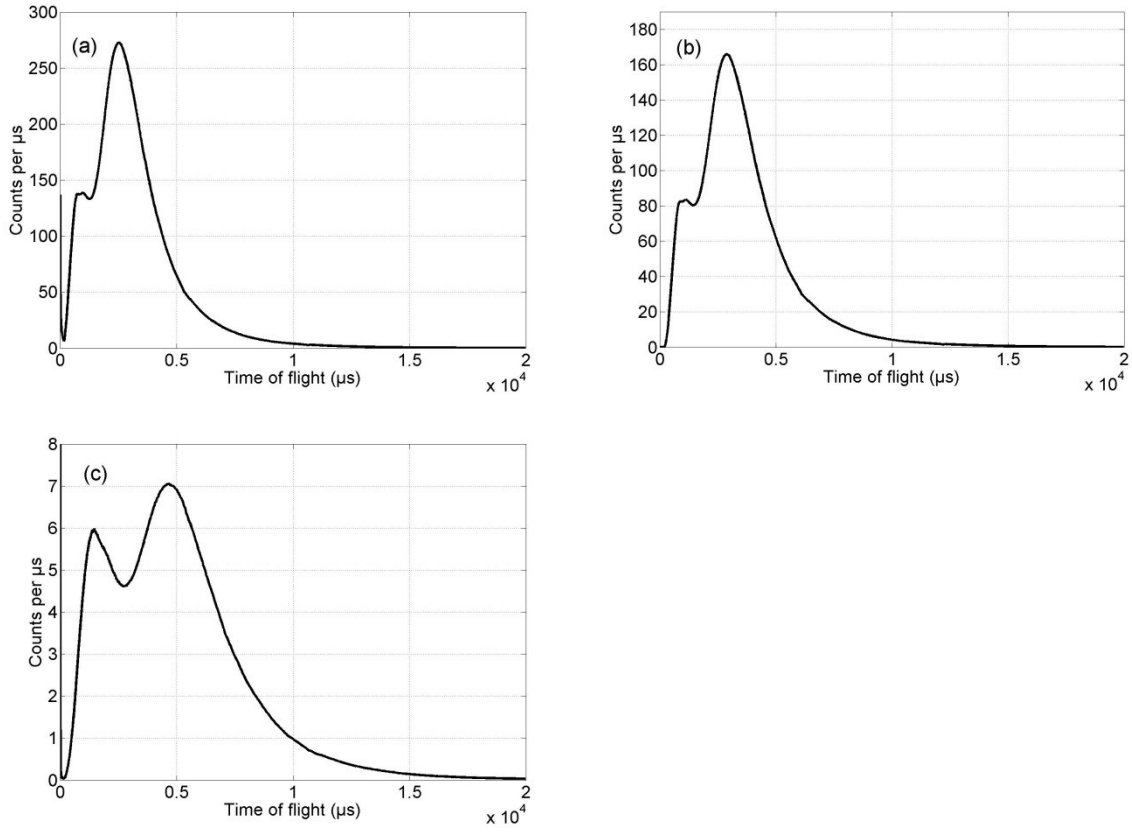

Figure 1: Measured flux as a function of time-of-flight from a standard white beam calibration measurement taken in cycle 16/1, before any problems with MAPS arose. (a) Data collected using monitor 1; (b) data collected using monitor 2; (c) data collected using a vanadium sample and the first 512 detector spectra

In figure 2 we show the same type of calibration measurements, taken at the beginning of cycle 16/3, using the same scale for all of the axes as in figure 1. The flux is clearly substantially suppressed in all monitors and detectors. In figure 3 we plot the ratio of the fluxes from before and after the problem, having converted the x-axis units from time-of-flight to neutron wavelength. To do this we use the formula $= 252.82\ L\ \lambda$, where *t* is time of flight in µs, *L* is the distance from the source to the detector or monitor in m, and λ is the neutron wavelength in Å. The fact that the ratios were the same as a function of wavelength for all of the monitors and detectors immediately suggested that the loss of flux was due to a physical object attenuating the beam, rather than the problem lying with the data acquisition electronics (DAE) or detectors – the DAE does not "know" the value of *L* in the above formula but the detectors and monitors have different flight paths. The above analysis also demonstrates that the problem must lie upstream of the first monitor.

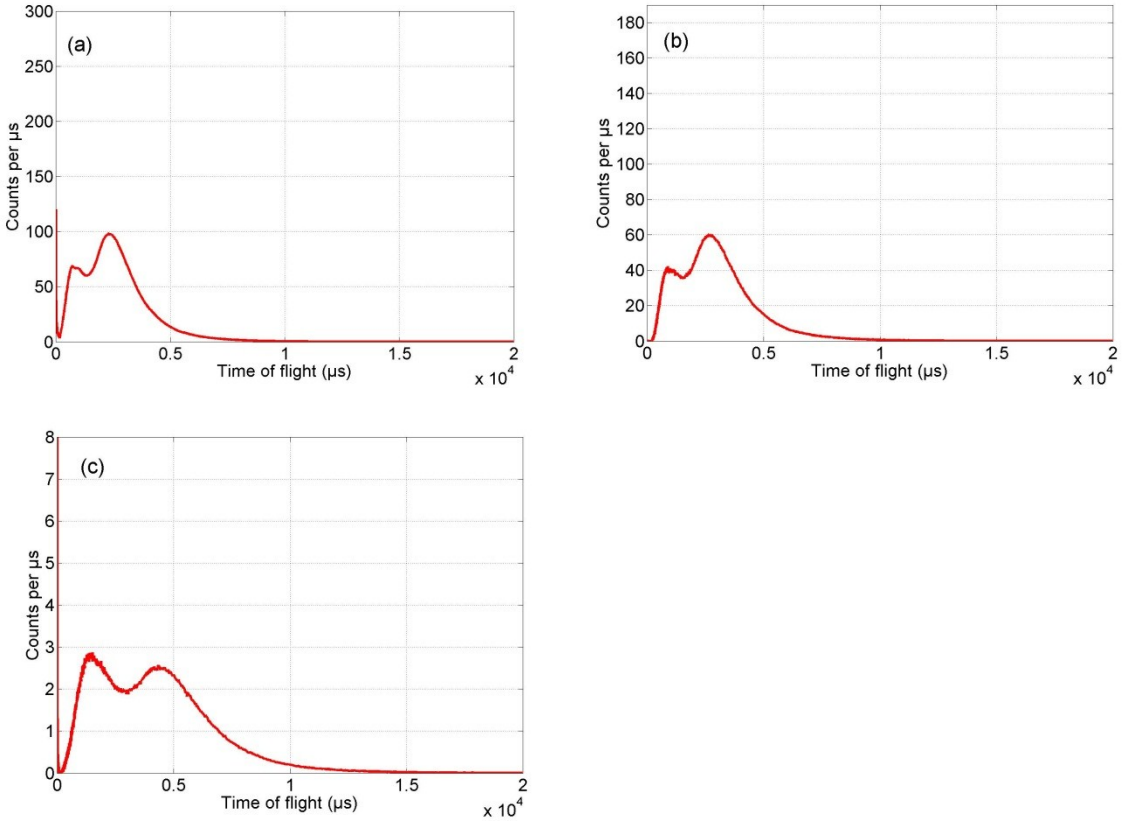

Figure 2: The same scheme of data as shown in figure 1, taken in cycle 16/3 after the problem arose.

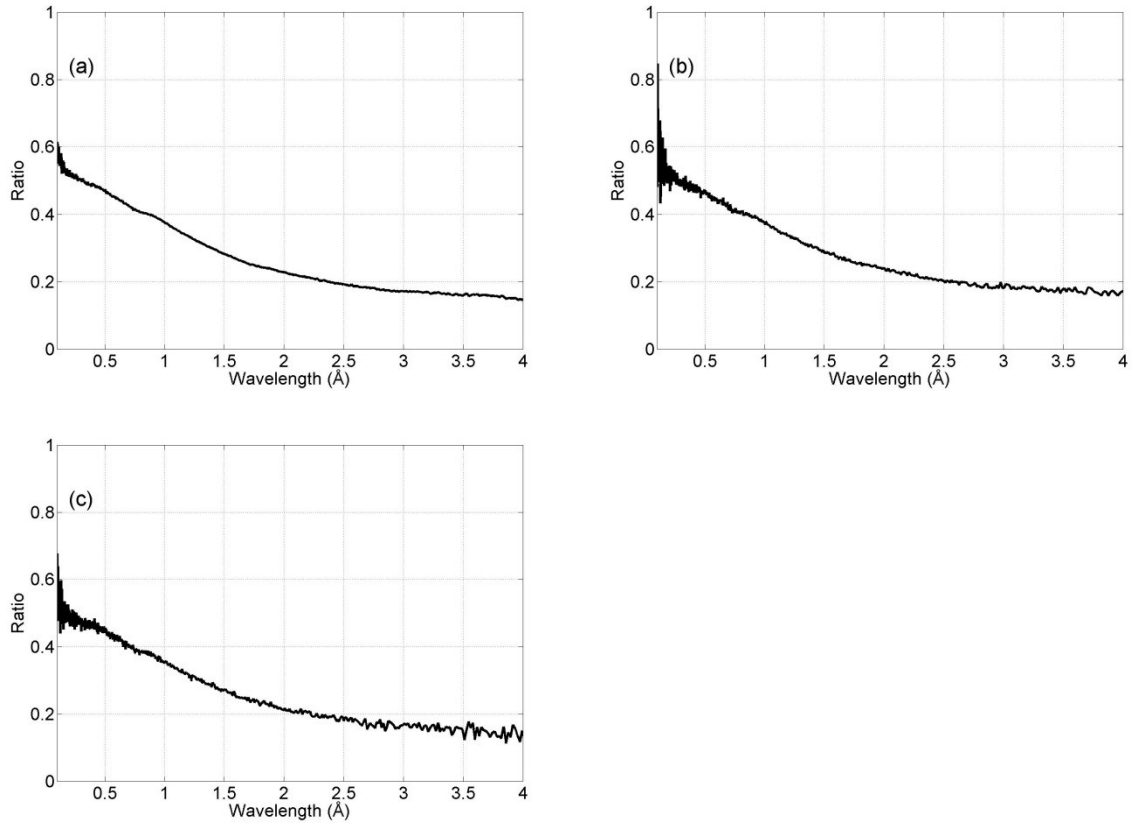

Figure 3: Flux ratio after the problem to before the problem, measured (a) in monitor 1; (b) in monitor 2; (c) in the detectors with a vanadium standard scatterer.

More complex investigations – a systematic survey of beamline components

In the following we describe investigations of all of the beamline components that were performed to confirm that they were working as expected and could therefore be ruled out as the cause of the problems. Results are presented in reverse order that the neutrons interact with them, i.e. starting at the data analysis and acquisition systems working back through detectors, sample, and collimation towards the target station. In figure 4 below we show a schematic view of MAPS, for orientation. Distances of components from the moderator centre, and beam apertures, are given in mm, and notable components are labelled.

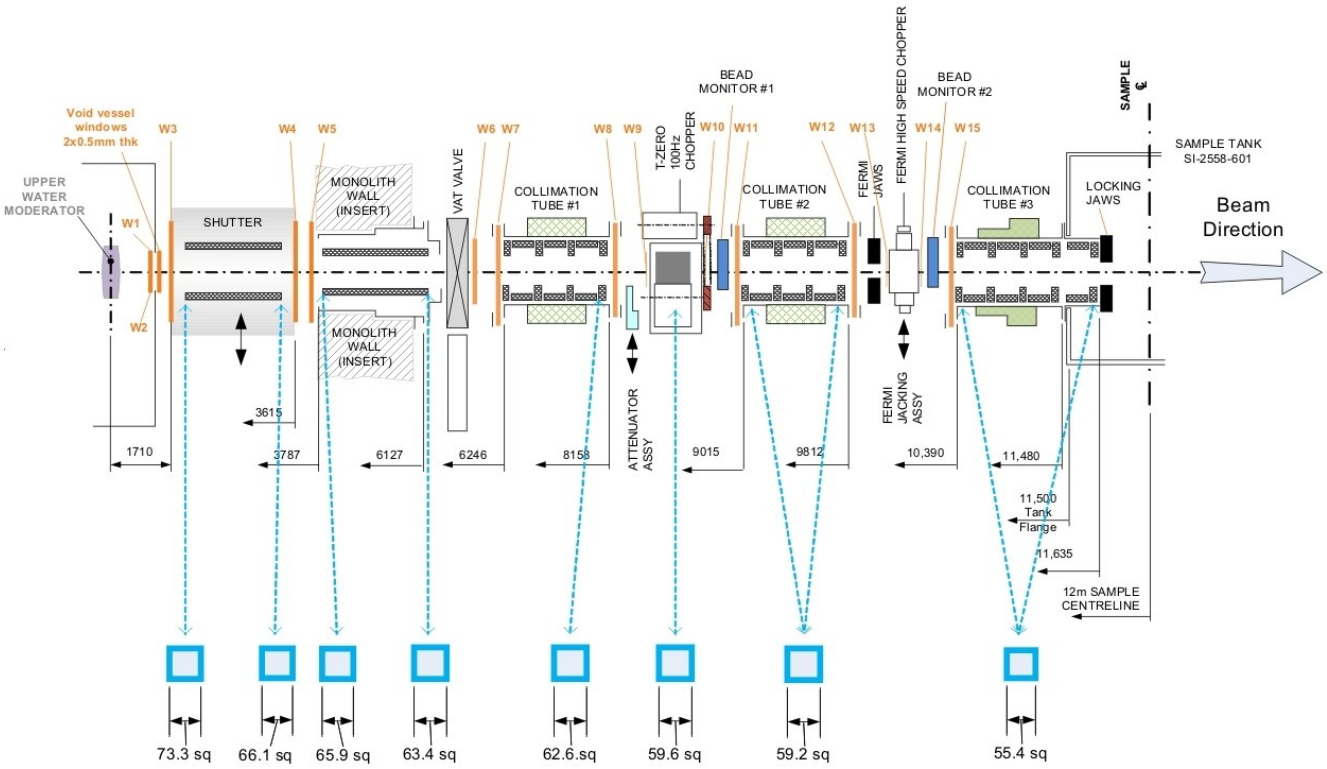

Figure 4: schematic of the MAPS beamline collimation and components, giving aperture sizes and distances from the source.

Data treatment / software

In order to illustrate that the problem was not simply a matter of bugs in data treatment algorithms, the raw data were processed and inspected by two different people, both using two different programs (Mantid and Matlab) to confirm the findings. The results were fully consistent no matter what program, or indeed computer operating system, was used. The results have already been shown in figures 1 – 3.

Data acquisition electronics and detector setup

Detector HT settings

If the detector HT settings were wrong then it is conceivable that the measured flux may be reduced in a non-uniform way. The HT settings were checked, and confirmed to be as they should be. To completely rule this out as a source of error the entire HT set was replaced with a spare. This made no difference to the measured flux.

DAE problems

As noted earlier, the fact that the neutron wavelength dependence of the flux attenuation is identical in different detectors located at different positions means that it is hard to imagine a situation in which the DAE would give rise to the problems observed. Nevertheless, the DAE was power cycled and inspected several times, to no effect. In addition a beam monitor that is independent of the DAE was used to measure the flux and compare to similar measurements that were performed with the same monitor when MAPS was functioning properly. The same wavelength dependent attenuation was observed as that seen with all of the MAPS detectors.

Another hypothesis was that a single detector was overloading and dead-timing the entire DAE. In principle the FIFO (first-in-first-out) veto on the acquisition system should prevent this, however to double check measurements of the signal on individual detectors using an oscilloscope were made. They were found to be consistent with those being recorded in the DAE, ruling this out as a possible source of the problem. Finally, a signal generator was connected to the DAE to inject a dummy signal with a known time structure, to check that the master pulse time on MAPS was correct and that the DAE response was as expected. Example measurements in which a signal generator was used to inject into the DAE are shown in figure 5 below. These results together indicate that the DAE was working correctly.

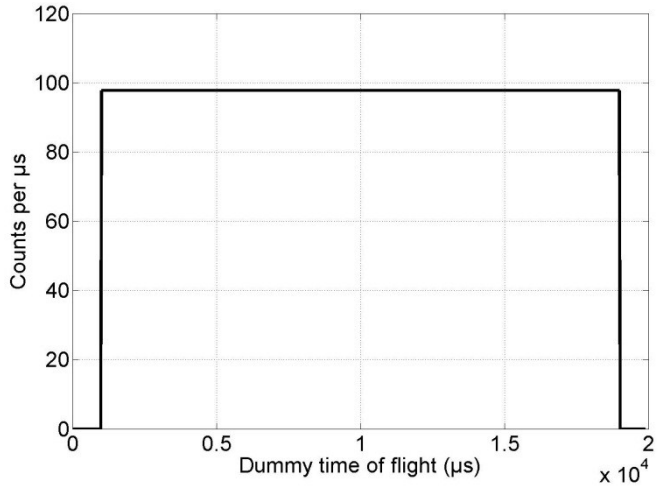

Figure 5: Signal measured in the monitor 2 channel when a fake square-wave signal was injected into the DAE, to test its response.

Sample and Fermi chopper

Both of these components can be trivially ruled out, since it was established that the problem was manifest in the monitor 1 signal and hence must lie upstream of its position. Monitor 1 is located at the downstream end of the t-zero chopper pit.

Inside the t-zero chopper pit

Monitor no. 1

Monitor 1 is the first detector that showed the reduced flux. If monitor 1's vertical position had slipped then scattering and / or absorbing material could be in the beam but a reduced signal still measured in this monitor and the other detectors. The position of monitor 1 did not appear to be wrong (see figure 6, right panel), however monitor 1 was removed from the beamline anyway and the flux re-measured, and no difference was observed in the remaining monitors and detectors.

T-zero chopper

Another piece of equipment upstream of the first monitor is the t-zero chopper itself. The entire chopper assembly was removed to check if this was the source of the problem. The flux reduction observed was the same as when the chopper was in place, thus ruling out the t-zero chopper as the source of beam attenuation.

Attenuator

At the upstream end of the MAPS t-zero chopper pit there is a beam attenuator (shown in figure 6, left panel), which is used when the instrument is being run in white beam mode and a strongly scattering single crystal sample is being aligned, to avoid detector overloading. The attenuator consists of two pieces of plastic of different thickness (5 mm and 10 mm respectively) to provide “mild” and “strong” attenuation, that are moved vertically into the beam by an actuator. The t-zero chopper pit was opened, the t-zero chopper removed to allow access, and the position of the attenuator measured in all three positions. It was found to be in the correct position, in particular with the “no attenuation” position corresponding correctly to the plastic nowhere near the beam. For certainty, the whole attenuator assembly was removed and measurements performed which showed no change in the reduced flux.

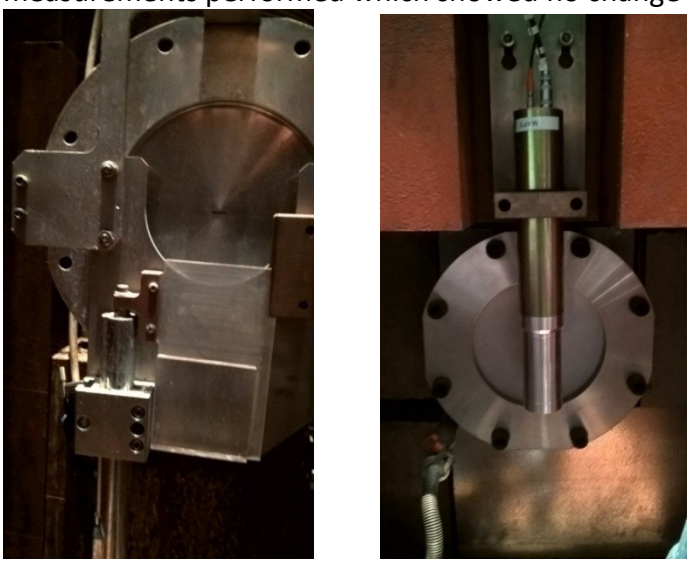

Figure 6: (left) Photograph of the beam attenuator, located at the upstream end of the t-zero chopper pit; (right) photograph of monitor 1, located at the downstream end of the t-zero chopper pit.

Collimation between VAT valve and t-zero chopper pit

To investigate whether there was any obstruction in the collimation which can be accessed comparatively easily with ISIS running and the shutter closed, the thin window at the upstream end of the chopper pit was opened. In figure 7 below is a photograph showing the inside of this collimation tube. The tube is clearly unobstructed, with undamaged B_4C collimation visible all the way up to the thin aluminium window at the upstream end.

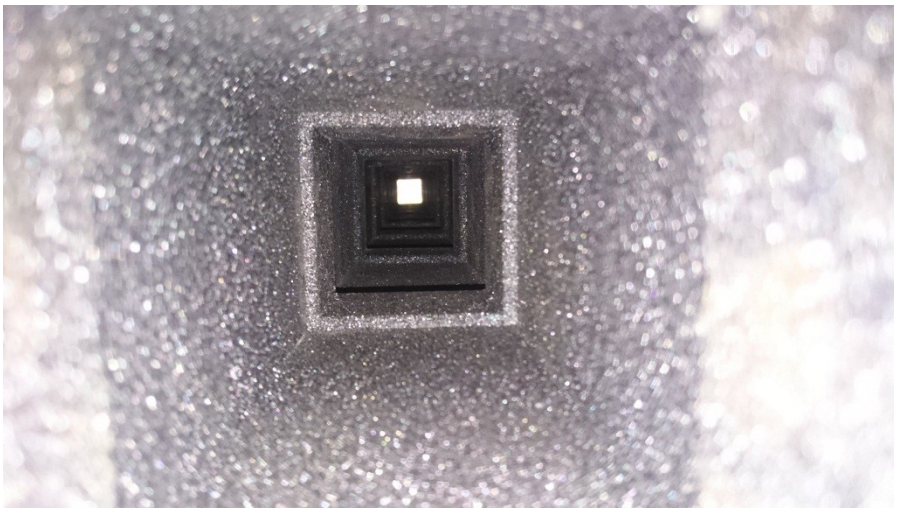

Figure 7: Photograph of the view through the collimation between the t-zero chopper pit and the VAT valve, viewed from the t-zero chopper pit end.

VAT valve

The VAT valve is situated at the downstream exit of the gun barrel collimation, after a thin aluminium vacuum window. If the VAT valve was closed the beam would be attenuated. However the actuator read-out on the VAT valve controller indicated it was in the correct position. Nevertheless measurements were made with it in the nominally open and closed positions, shown as a ratio in figure 8 below as a function of neutron wavelength. With the VAT valve closed the flux is attenuated still further, and though the data are rather noisy due to the short measurement duration, it is clear the structure with a dip around 3.5 Å is rather different to that observed otherwise.

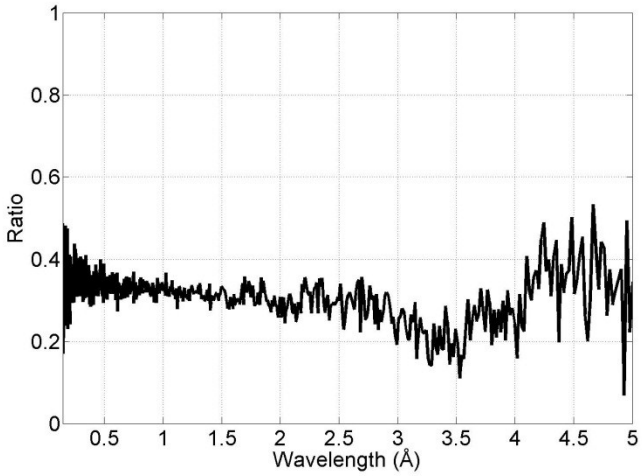

Figure 8: Ratio of the flux when the VAT valve is closed to when it is open, measured in monitor 1.

There is a small gap between the VAT valve and the collimation that runs from the monolith to the chopper pit. The shielding was removed to investigate whether anything was obstructing the beam at this position. As can be seen in figure 9 below, there was no obstruction there. It should also be noted that the VAT was removed and replaced in the shutdown between cycles 16/3 and 16/4, as part of planned routine maintenance. This made no difference to the measured flux.

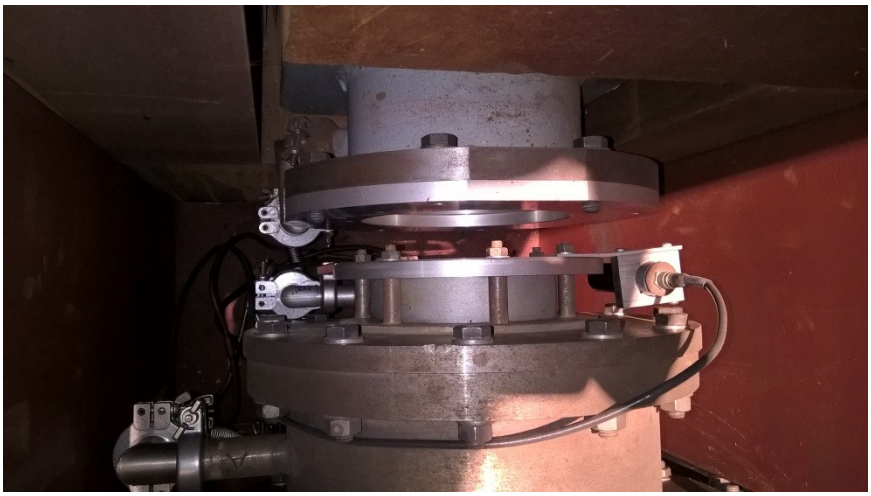

Figure 9: Photograph of the VAT valve, viewed from above. The beam direction is down in this image.

Insert / "gun barrel"

This comprises a steel housing containing a collimation tube. The collimation consists of a square cross-section cut from thick disks of B_4C crispy mix. These disks are glued to a steel housing, around which is further shielding comprising Borax (sodium tetraboride and resin) and iron shot. Visual inspection of this area was performed after removing a large amount of shielding from MAPS and adjacent beamlines, so was done in the short shutdown between cycles 16/3 and 16/4. Figure 10 below shows the view through the collimation, with no obstruction visible.

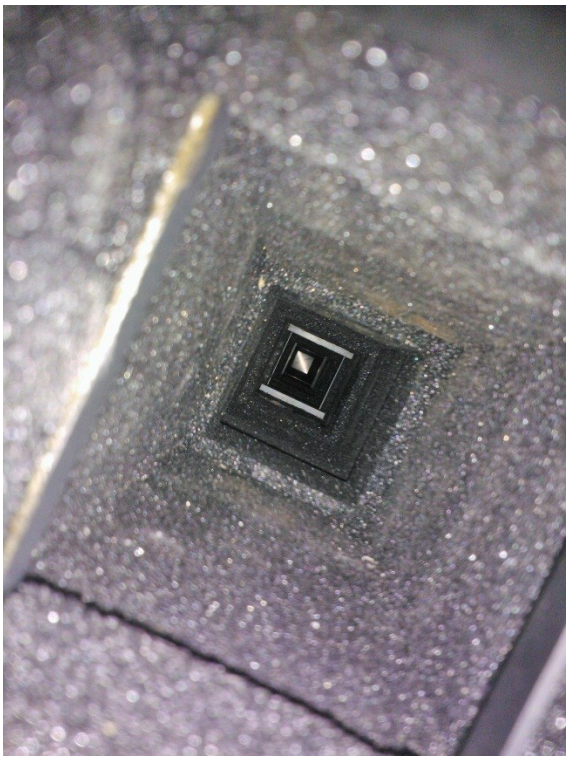

Figure 10: Photograph of the view through the collimation in the insert, viewed from the VAT valve end.

Shutter

Shutter position

Very rarely the vertical position calibration of the shutters of TS-1 can drift. A scan of the shutter position was performed, shown in figure 11 below. The shutter was found to be already at the optimal position of peak flux (indicated by the black vertical line) and consequently the vertical position of the shutter could be ruled out as the source of the problem.

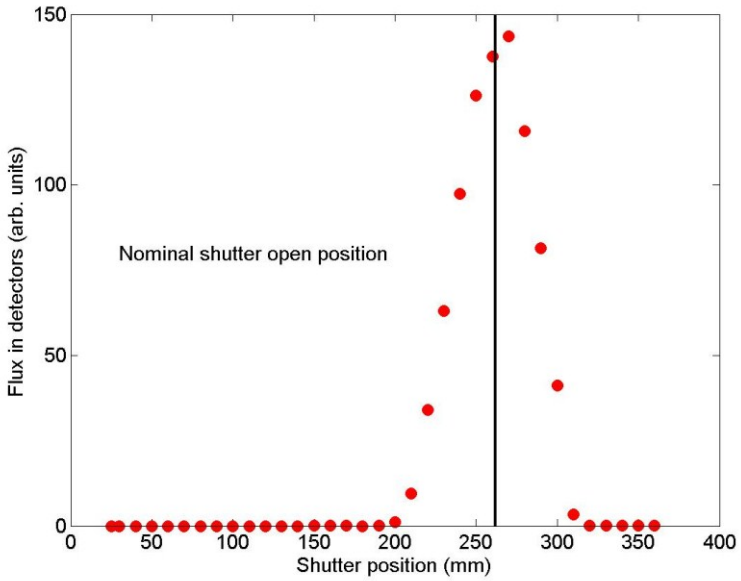

Figure 11: The flux measured in the detectors from the standard vanadium sample as a function of shutter position. The vertical black line indicates the nominal open position.

Shutter obstruction

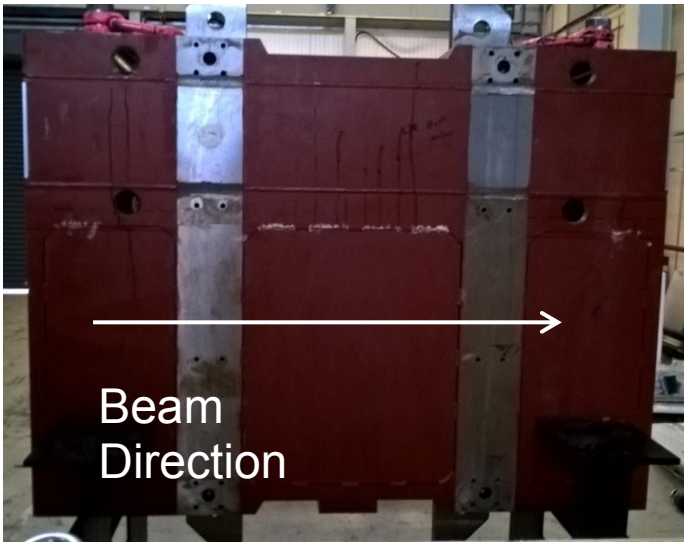

The shutter on MAPS was installed in the late 1990s and has seen a huge amount of radiation in years since. Removal of such shutters is a complex task, taking several weeks, and the expected dose rate on the shutter would prohibit manual inspection. Therefore an obstruction inside the shutter cannot be manually checked, though it may be inferred through indirect measurements (discussed later). A photograph of a shutter (not the MAPS one) is shown in figure 12, for reference, with the beam direction indicated.

Figure 12: Photograph of a shutter (not the MAPS one), with beam direction indicated.

Void vessel

The target and moderator assembly are located inside a stainless steel chamber known as the void vessel, which is flooded with helium gas during operation of ISIS. Engineering drawings show that there is a shelf located inside the void vessel 9approx. 300mm below the double-walled aluminium window between the void vessel and the MAPS shutter entrance. It is conceivable that an object may fall on to this shelf in such a way as to obscure the view of MAPS to the target station. However, the void vessel is extremely difficult,

if not impossible, to access even with remote inspection methods. Investigations of this area were not performed.

Moderator and target assembly

This was an early suspicion as the source of the flux loss. Between cycle 16/1 and 16/3 (in cycle 16/2 beam was only delivered to TS-2, and not to TS-1) the target, reflector and moderator (TRAM) assembly was pulled back and the water moderator viewed solely by MERLIN was replaced. It was the only component of MAPS that was known to have undergone any perturbation in this period.

However, if there was a problem with the moderator viewed by MAPS one would expect the flux to be different from normal on other beamlines that view the same water moderator. These are SXD and VESUVIO on the south side, and TOSCA, INES and POLARIS on the north side. Analysis of the data from calibration standards taken on VESUVIO, SXD and POLARIS indicated no change in the flux measured on those beamlines. TOSCA and INES were not operating at the time of these measurements due to an upgrade to install neutron guides. This indicated that there was no global problem with the TS-1 water moderator.

It was suggested that a highly localised problem with the target and moderator assembly might account for the reduced flux, for example a slight mis-positioning of the TRAM, to which MAPS would be more susceptible due to its line of sight being bounded by the reflector (see figure 13 below). To assess this, the TRAM was pulled back in the short shutdown between cycle 16/3 and 16/4. Nothing out of the ordinary was observed, and after the TRAM was returned to its operating position the flux measured on all beamlines was the same as in cycle 16/3.

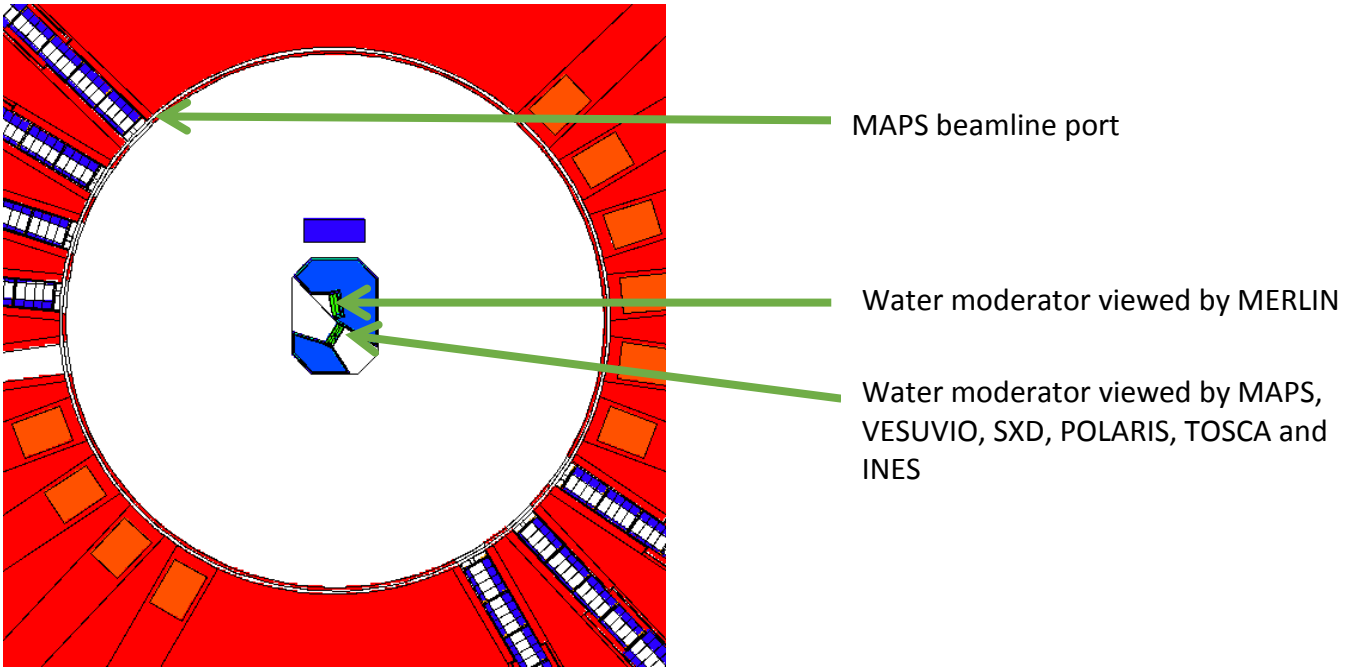

Figure 13: Schematic view of the void vessel, showing the upper water moderators and several beam ports.

Detailed analysis of the neutron spectra and neutronic simulations

Type of material in the beam

Following on from the above analysis of the VAT valve, it was noted that if any crystalline material (i.e. metal) was obstructing the beam then characteristic Bragg edges would be visible. Only tiny Bragg edges were observed, which arise from the thin aluminium windows between isolated vacuum sections and have always been present on MAPS. This indicated that the beam was being obscured by something amorphous, e.g. wax, plastic, etc. rather than crystalline. We can illustrate this by examining the flux reduction when the plastic attenuator is used, shown by the black curve in figure 14 below, and comparing to the flux reduction problem, shown by the red curve. The wavelength dependence, and indeed the magnitude of the reduction in flux, is qualitatively very similar in both cases.

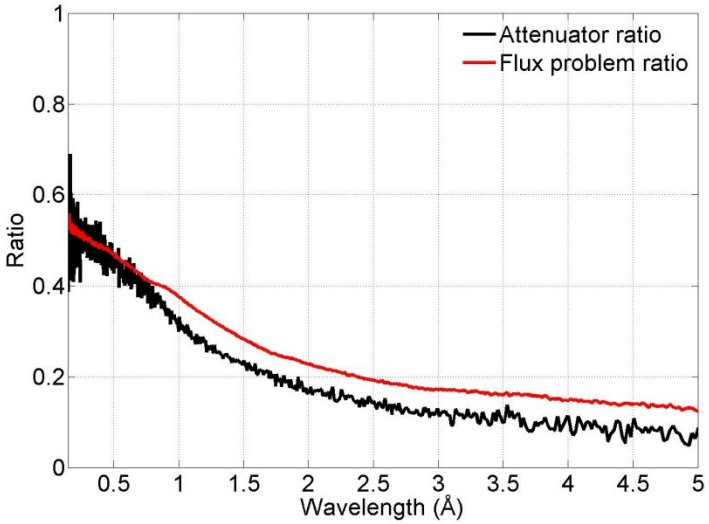

Figure 14: Comparison of the attenuation of the beam by the plastic attenuator (black curve) with the attenuation caused by the flux problem (red curve).

We also performed a more detailed analysis of the high energy (i.e. short time-of-flight) neutron spectrum. We found several absorption features due to nuclear resonances, however these are largely the same as those seen in data taken before the problems. They most likely arise from alloying materials used in the aluminium thin windows.

Attenuation spectrum with the shutter part-closed

A measurement of the flux with the shutter 80% closed was performed, to compare the wavelength dependence of the flux reduction due to that with the problem flux reduction. The effect of part-closing the shutter on the wavelength-dependent attenuation is shown in figure 15 below. At long wavelengths the transmission is approx. 20%, which is what would be expected. There is a small upturn in transmission for wavelengths < 0.25 Å, the origin of which is unclear.

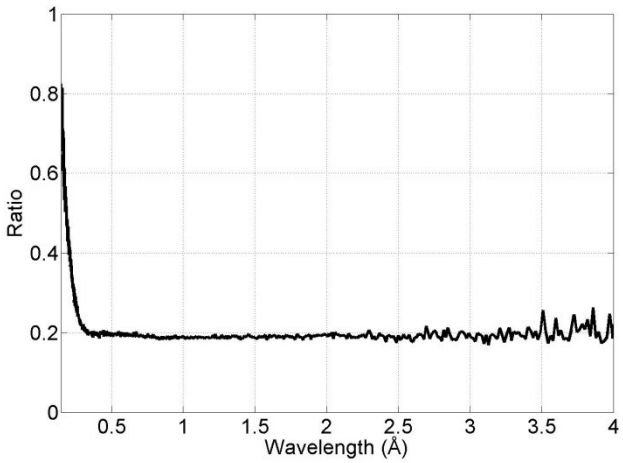

Figure 15: Ratio of the flux measured in monitor 2 for the shutter 80% closed to its fully open position.

Neutronics from the TS-1 baseline model

As part of the TS-1 upgrade project detailed neutronic models had already been constructed of the flux from all of the moderators as viewed from all of the beam ports. Additional material could be added to these models to simulate their effect on the flux measured on MAPS. In figure 16(a) simulations of the attenuation due to the presence of borated polythene of various thicknesses are shown. In figure 16(b) similar simulations are shown for borated steel. Note the clear Bragg edge around 3-4 Å that is not seen experimentally. Unfortunately these simulations are only indicative, there are lots of combinations of materials that could be attenuating the beam and the most that can be said is that the measurements are consistent with simulations thereof.

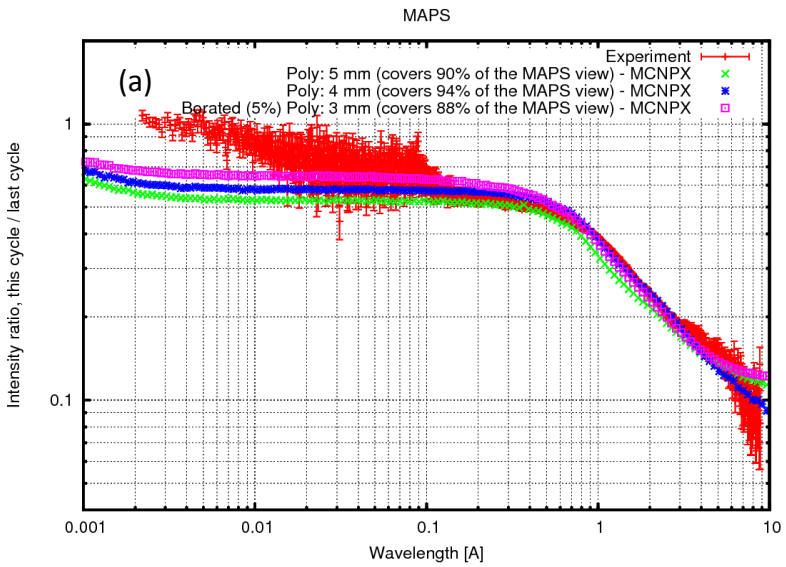

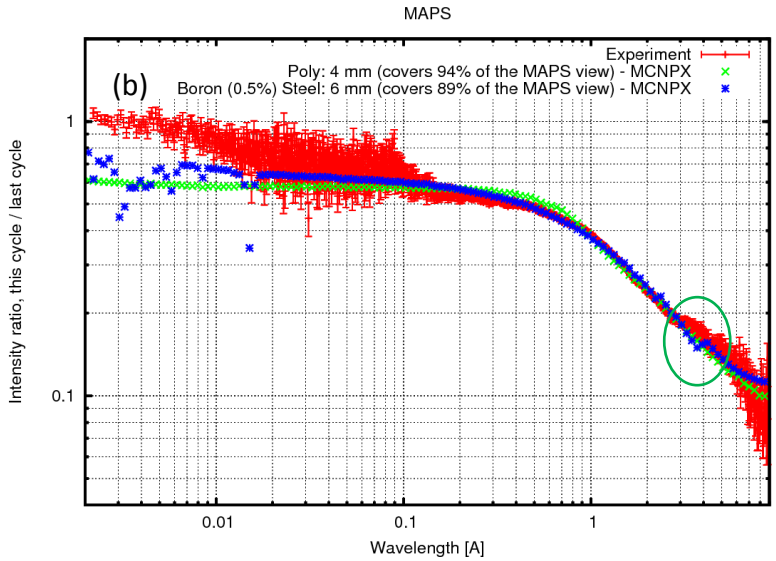

Figure 16: Neutronic simulations from the TS-1 baseline model with extra materials added to simulate their attenuation (plotted). (a) Comparison of attenuation due to polythene covering various fractions of the beam with the measured flux reduction; (b) Comparison of attenuation due to polythene and borated steel with the measured flux reduction.

Beam profile measurements

The beam profile at the sample position was measured using an nGEM detector. This is a 2D neutron detector with an active area of 100x100 mm^2 and a pixel size of 0.8x0.8 mm^2. It uses a 100 nm layer of $^{10}B_4C$ as a neutron converter providing an efficiency of 10^{-4} at 1 Å. It is able to operate up to a total count rate of 10 MHz on the whole detector area. It is commercialised by BeeBeans [2]. A representative image for neutrons with wavelength 1 Å (images at other wavelengths look the same) is shown in figure 17 below. To illustrate the effect on the beam profile of an obstruction the shutter may be partially closed by various amounts. Measurements were performed with the shutter fully open (panel a), 80% open (b), 50% open (c), and 30% open (d). These illustrate that the beam divergence is such that even for the shutter mostly closed the beam profile at the sample position is fairly uniform.

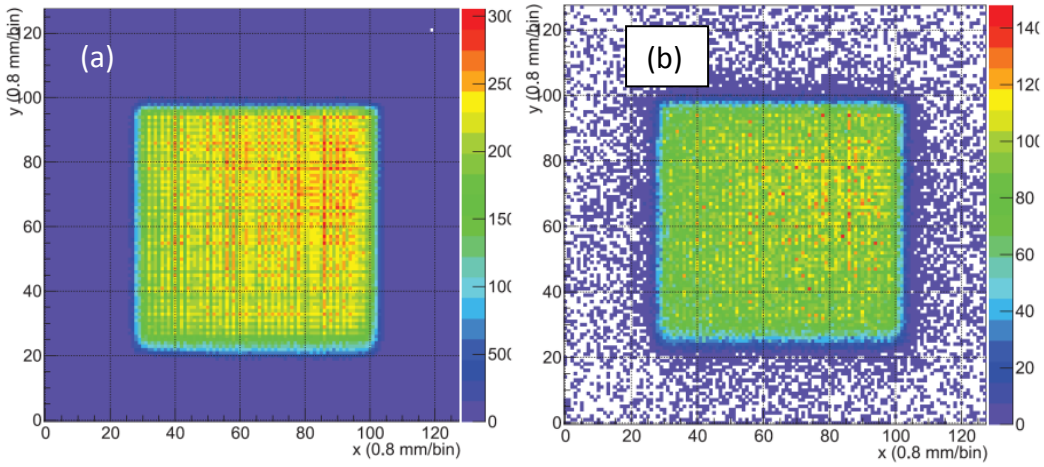

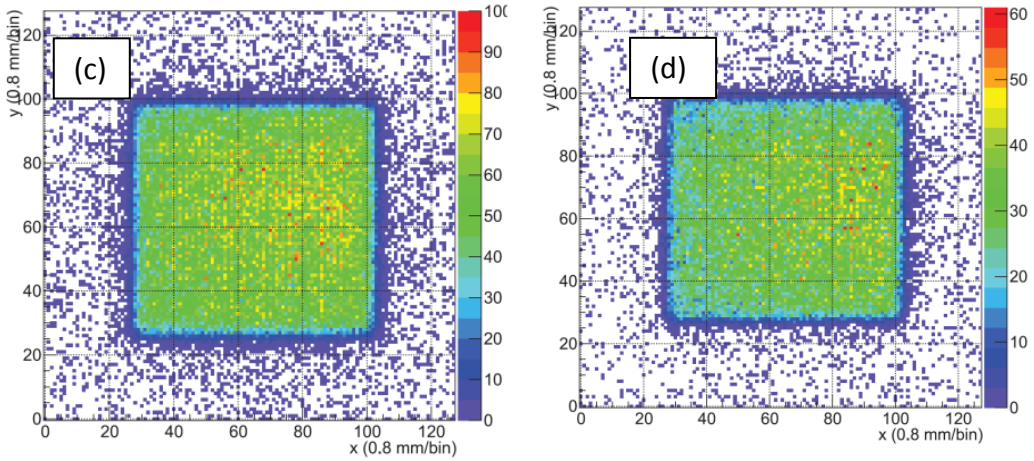

Figure 17: Beam profile measured at the MAPS sample position with an nGEM position-sensitive detector and the shutter in various positions. (a) Shutter fully open; (b) shutter 80% open; (c) shutter 50% open; (d) shutter 30% open. Note that each plot uses a different colour scale, but that the plots are normalised to counting time, so that the numerical intensities can be compared.

McStas simulations of the beam profile

If a strong absorber (e.g. B_4C) or a scatterer (e.g. hydrogenous material) had become dislodged in the upstream collimation we would expect to see a shadow in a measurement of the beam profile. This can be simulated using the McStas software [1], and the results of such simulations are shown below in figure 18. The top left panel shows the beam profile simulation with no obstructions. The top right panel shows the profile if an attenuator covers half of the beam area at the entrance to the shutter. The bottom left panel shows the beam profile if an attenuator covers half of the beam area at the exit of the shutter. The bottom right panel shows the beam profile if an attenuator covers half of the beam area at the exit of the gun barrel collimation.

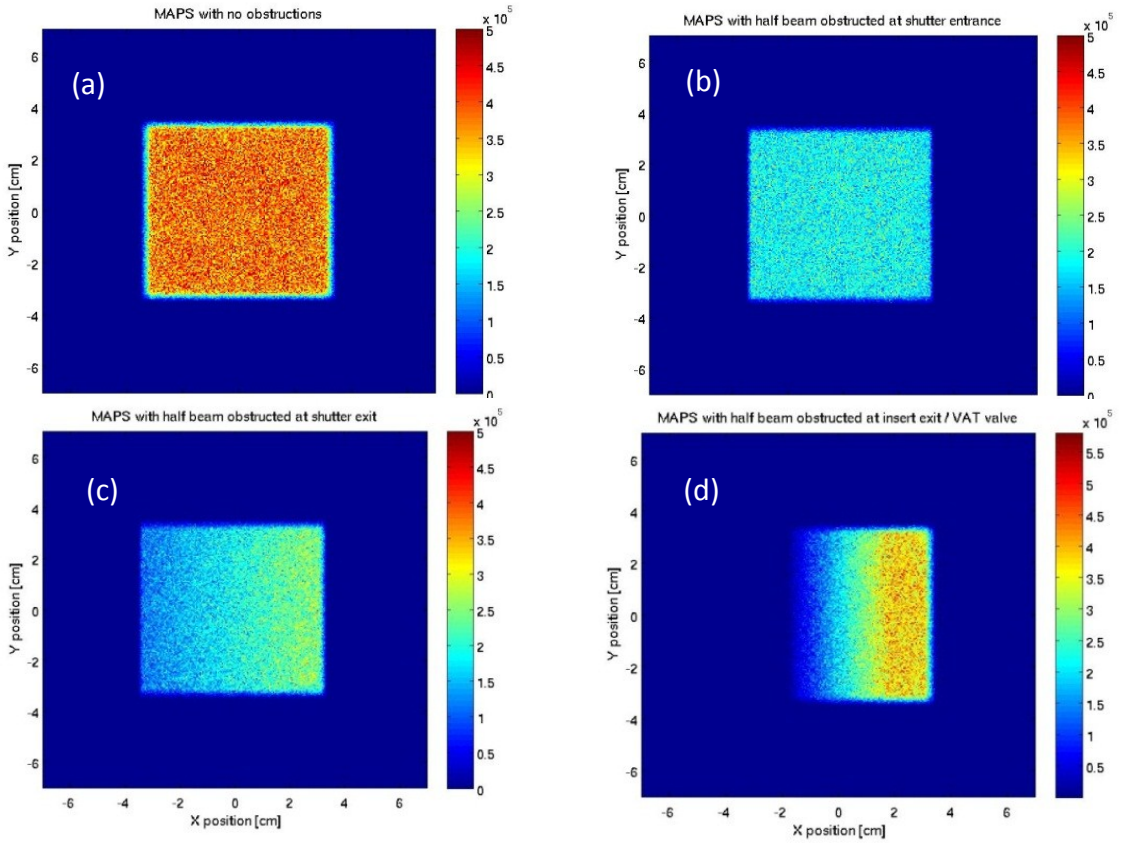

Figure 18: McStas simulations of the beam profile at the sample position with a perfect absorber covering half of the beam at various different positions along the collimation. (a) Simulated profile with no obstructions; (b) simulated profile with an obstruction at the entrance to the shutter; (c) simulated profile with an obstruction at the exit of the shutter; (d) simulated profile with an obstruction at the exit of the insert.

These simulations indicate that if an attenuator was obstructing half the beam then it would only cast a shadow / give a notably inhomogeneous beam profile if it were downstream of the exit of the shutter. The calculations are consistent with the data collected with the shutter partially closed, in which a uniform beam profile was observed. This would then imply that any obstruction on MAPS must also lie sufficiently far upstream from the sample that the beam divergence results in the uniform profile observed.

Pinhole camera measurements

Using another nGEM detector at the sample position (12 m from the source), a 0.5 mm diameter pinhole in a sheet of cadmium was placed in the beam centre at the upstream end of the t-zero pit (approx. 8.2 m from the source). An nGEM with a higher efficiency (5% at 1 Å) was used for these measurements compared to that used for measuring the beam profile, to reduce the collection time since only a tiny fraction of the incident neutrons pass through the pin-hole.

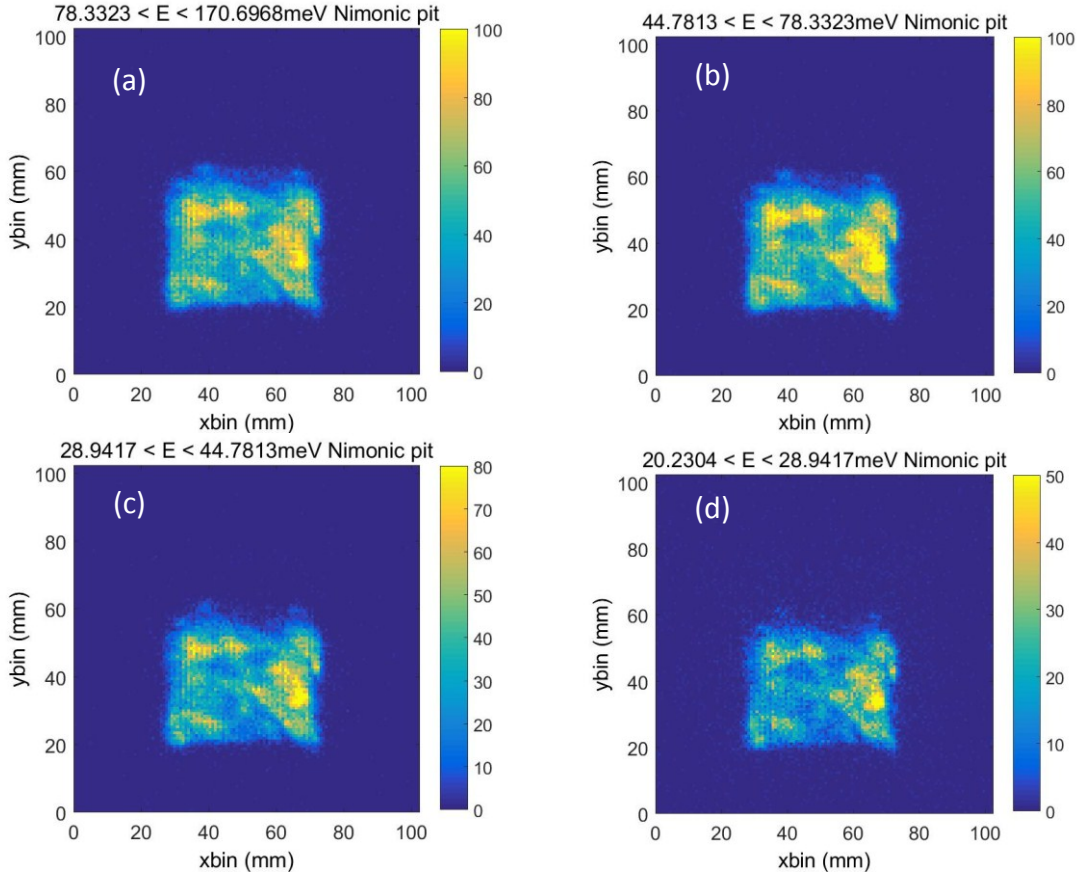

Figure 19: Pinhole camera images of the water moderator viewed by MAPS, using an nGEM detector at the sample position and a pinhole 8.2 m from the source. (a) Image for neutron energies in the range 78.3 < E < 170.7 meV; (b) image for neutron energies in the range 44.8 < E < 78.3 meV; (c) image for neutron energies in the range 28.9 < E < 44.8 meV; (d) image for neutron energies in the range 20.2 < E < 28.9 meV.

The image size and spatial resolution for a pinhole camera can be easily calculated (see appendix). The image on the nGEM detector should be 42.9 mm square, assuming a moderator of size 120 mm square and a view through the beamline collimation as shown in figure 4. The spatial resolution, i.e. the size of object at the source that may be resolved, was calculated to be 3.2 mm. Images collected as a function of neutron energy are shown in figure 19 below, for a selection of energy windows below 200 meV (i.e. below the cadmium cut-off).

The highly inhomogeneous image of the source seen in figure 19 indicates that, as expected, there is a highly structured physical obstruction in the beamline. This obstruction must lie upstream of the gun barrel collimation, since visual checks found nothing downstream of this point and the beam profile measurements would also suggest this. For confirmation of this analysis we show in figure 20 below similar pinhole camera measurement performed on VESUVIO, which is adjacent to MAPS and views the same moderator face. The images are rounded because the collimation tubes on VESUVIO are circular in cross-section, rather than square.

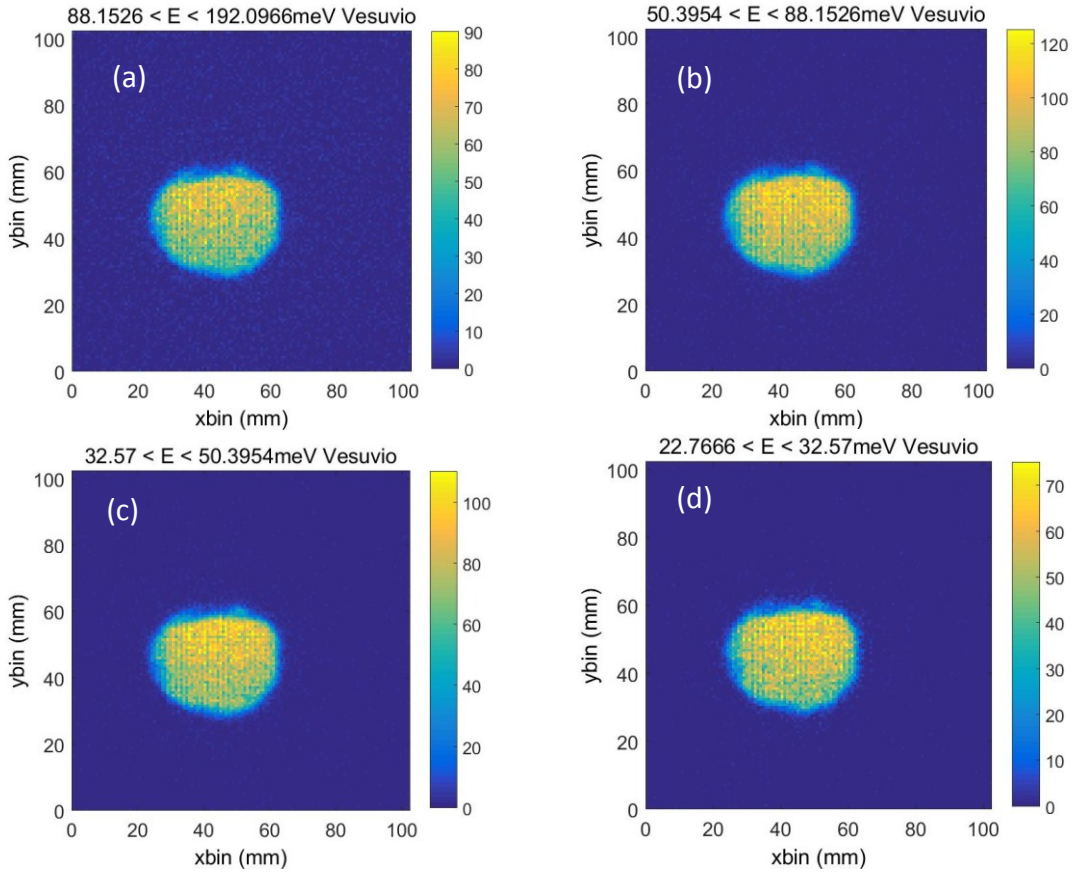

Figure 20: Pinhole camera images of the water moderator viewed by VESUVIO, the same moderator face as viewed by MAPS. (a) Image for neutron energies in the range 88.2 < E < 192 meV; (b) image for neutron energies in the range 50.4 < E < 88.2 meV; (c) image for neutron energies in the range 32.6 < E < 50.4 meV; (d) image for neutron energies in the range 22.8 < E < 32.6 meV.

Note that the profile measured on VESUVIO shows a slight increase of intensity towards the top of the image. This is to be expected – the image on a pinhole camera is inverted, so this indicates that the flux from the moderator is larger at the bottom than at the top. The moderator is above the target, and we would expect higher flux from the target side of the moderator.
An nGEM with a higher efficiency (5% at 1 Å) was used for these measurements to reduce the collection time since only few neutron/frame pass through the pin-hole.

Shutter replacement

In the ISIS shutdown in April 2017 the MAPS shutter was replaced. Due to a planned upgrade to the instrument involving replacement of the instrument collimation with neutron guides, for which all of the components had already been bought, a replacement shutter was available. It had a larger aperture than the old shutter (94 x 94 mm compared to 73.2 x 73.2 mm for the original shutter), and on the basis of ray-tracing simulations it would be expected to provide an increase in flux of approx. 35% due to the fact that the wider aperture would be viewed through the original collimation downstream of the shutter. In figure 21 below we show as a function of neutron wavelength the measured flux in monitor 2 (panel (a)) in the detectors with the vanadium standard sample (panel (b))[1]. Data are shown for cycle 16/1 (before the problem arose, black), cycle 16/3 (when the problem first arose, red) and cycle 17/1 (after the shutter was replaced, blue).

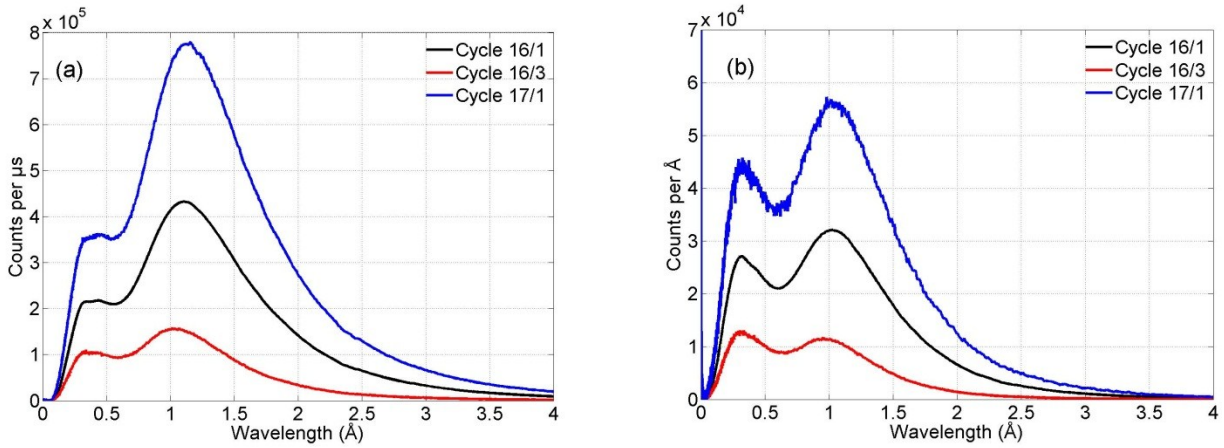

Figure 21: Flux as a function of wavelength measured in cycle 16/1 (black curves), cycle 16/3 (red curves) and cycle 17/1 after the shutter replacement (blue curves). Data shown measured (a) monitor 2; (b) a standard vanadium sample scattering into the detectors.

It is clear from the above data that replacing the shutter fixed the problem. Indeed, the gain in flux was more than expected on the basis of McStas ray-tracing, 75% obtained as opposed to 35% calculated, which suggests that there may have always been problems with the original shutter, but that these were minor and hence not noticed.

The precise nature of the obstruction in the shutter that caused the flux problem cannot be directly investigated at the time of writing. When the original shutter was removed it was found to be highly radioactive, and was transferred to a steel storage flask and thence to the active material storage area in building R40. Until such time as a remote handling option can be devised direct investigations of the shutter cannot be safely conducted.

Conclusions

The MAPS beam was being strongly attenuated, to a disruptively high level to the user programme, by an obstruction in the shutter. Replacement of the shutter resulted in the solution of the problem, though the precise cause of the problem cannot be confirmed until direct investigation of the (radioactive) shutter can be undertaken. On the basis of neutronic simulations and comparisons with data taken with a plastic attenuator in the beam it is suspected that the source of the problem was a hydrogenous scatterer of

[1] Monitor 1 had been disconnected as part of the beamline investigations and had not been reinstalled at the time of these measurements.

neutrons. After more straightforward checks had been performed it was found that the most informative measurements to diagnose the problem involved the use of a pinhole camera setup that allowed the source's flux homogeneity to be probed.

References

[1] P. Willendrup, E. Farhi and K. Lefmann, Physica B **350,** 735 (2004)
[2] https://www.bbtech.co.jp/en/

Appendix – image size and resolution of a pinhole camera

Consider a source of size *y* a distance *x* from a pinhole of diameter *d,* and an image plate a distance *x'* from the pinhole. The size of the image of the source on the plate *y'* is given by,

$$\frac{x'}{x} = \frac{y'}{y}.$$

If we have a point source then its image will be projected on to the image plate as a circle of diameter *D*, given by,

$$D = \frac{d\ (x + x')}{x}.$$

Therefore the resolution, i.e. to distinguish between two points separated by a distance *R* on an extended source, is given by,

$$R = \frac{2\ D\ x}{x'} = \frac{2\ d\ (x + x')}{x'}.$$